(Received 3 August 2025, Accepted 3 September 2025, Scheduled 9 September 2025)

Single-Cavity Triple-Mode Bandpass Filter Based on a Novel Combined-Type Rectangular Patch Resonator

Yaoran Yue and Yang Liu*

Sichuan University-Pittsburgh Institute, Sichuan University, Chengdu 610207, Sichuan, China

ABSTRACT: A novel single-cavity triple-mode combined-type rectangular patch resonator (CRPR) is proposed in this paper, which is realized by integrating the rectangular patch structure with a rectangular substrate integrated waveguide (RSIW) structure. By cleverly designing the length-to-width ratios of both the RSIW structure and patch structure, as well as the size ratio between them, the three higher-order modes of the CRPR can be resonance. Then, a highly selective bandpass filter (BPF) is realized through a special feeding structure. To demonstrate the method, an instance of a BPF is designed, synthesized, fabricated, and measured. The consistency of all results validates the effectiveness of the proposed design method. The proposed filter offers advantages such as relatively compact size, easy integration, and high selectivity.

1. INTRODUCTION

Planar bandpass filter (BPF) is an essential component in radio frequency (RF) front-end systems, and due to its advantages such as easy integration and compact size, it has become a focus of widespread attention and research. Planar BPFs with multiple finite-frequency transmission zeros (FTZs) are realized using single-mode microstrip lines, patches, and substrate integrated waveguide (SIW) structures, respectively [1–4]. Compared to single-mode resonators, dual-mode resonators can support two resonant modes within a single physical cavity, replacing two single-mode single cavities, thereby enabling the realization of more compact BPFs [5–8]. They are also commonly used methods for implementing BPFs.

Compared to single- and dual-mode BPFs, single-cavity triple-mode BPF can theoretically achieve a more compact size by reducing the physical number of resonators, eliminate the need for additional physical coupling paths to achieve lower loss, and improve selectivity by using a single cavity to implement higher-order BPFs [8–11]. In addition, the implementation of planar cavity multi-mode resonators has made the combination-type multimode resonator technology one of the current research hotspots. By etching additional planar circuit structures on the metal surface of SIWs or patches, or by introducing additional coupling structures inside the planar cavity, the space of planar resonators can be fully utilized to design compact and low-loss BPFs [12–14].

In this paper, the characteristics of rectangular patch and SIW resonators are analyzed in detail and effectively utilized. By cleverly using their respective length-to-width ratios and the size ratio between the two, a novel single-cavity triple-mode combination-type rectangular patch resonator (CRPR) is achieved. Using the CRPR and feeding structure, a BPF with two FTZs is realized, enabling effective control over the frequency locations of the FTZs and bandwidth (BW). Subsequently, a BPF example with a center frequency (f_0) of 5.35 GHz and a BW of 610 MH is designed. The validity of the proposed filter design theory is verified through simulation, coupling matrix synthesized, physical fabrication, and vector network analyzer measurement. The proposed BPF exhibits relatively easy integration, compact size, and high selectivity.

* Corresponding author: Yang Liu (scu2023jacky@163.com).

2. ANALYSIS OF THE PROPOSED SINGLE-CAVITY TRIPLE-MODE CRPR

The 3-D view of the CRPR is shown in Fig. 1(a), which is a five-layer structure. The first, third, and fifth layers consist of copper, while the second and fourth layers are substrate layers. The third and fifth layers are connected through metallized blind vias that pass through the fourth layer. Fig. 1(b) shows the top view of the CRPR, where the red areas represent the rectangular SIW (RSIW) structure, and the yellow areas indicate the patch structure. The upper and lower metal layers of the entire CRPR can be regarded as electric walls, while the remaining sides can be viewed as magnetic walls. Therefore, it is overall considered a patch resonator. Define the length and width of the CRPR as L and W, respectively, and the length and width of the RSIW as L_3 and W_3, respectively. The diameter and spacing of the blind vias in the RSIW are defined as d_1 and d_2, respectively. The initial resonant frequency of the patch and RSIW can be approximately calculated as [5, 6, 13, 14]:

$$f_{\mathrm{TE}_{mn0}} = \frac{c}{2\sqrt{\mu_r \varepsilon_r}} \sqrt{\left(\frac{m}{L_e}\right)^2 + \left(\frac{n}{W_e}\right)^2} \tag{1}$$

$$L_e = L - \frac{d_1^2}{0.95 \times d_2}, \quad W_e = W - \frac{d_1^2}{0.95 \times d_2} \tag{2}$$

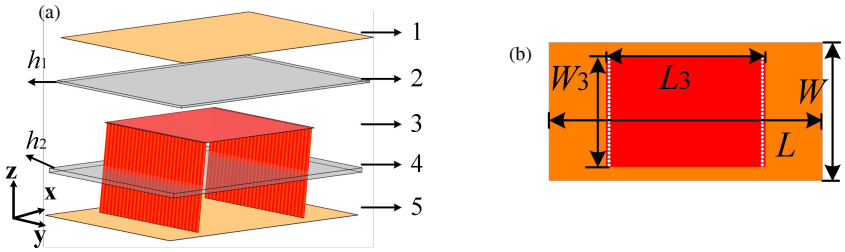

FIGURE 1. Configuration of the proposed triple-mode CRPR (yellow or red: copper, white: metallized blind vias, gray: dielectric substrates). (a) 3-D view. (b) Top view.

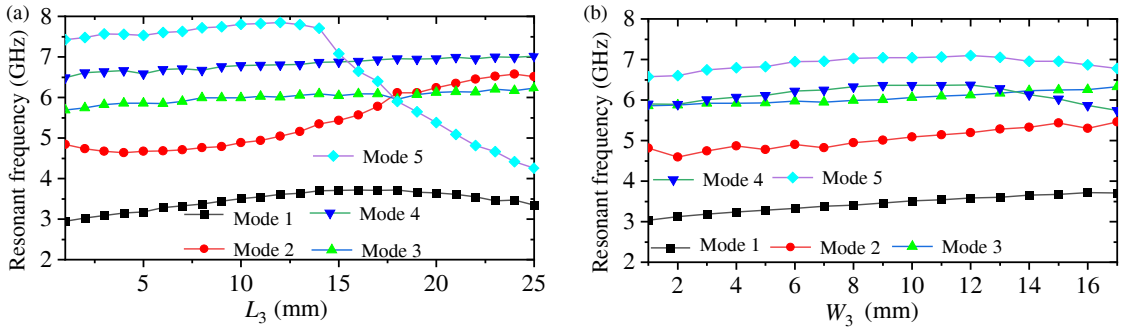

FIGURE 2. Resonant frequencies of the first five modes in the CRPR by changing L_3 and W_3, respectively. (a) L_3. (b) W_3.

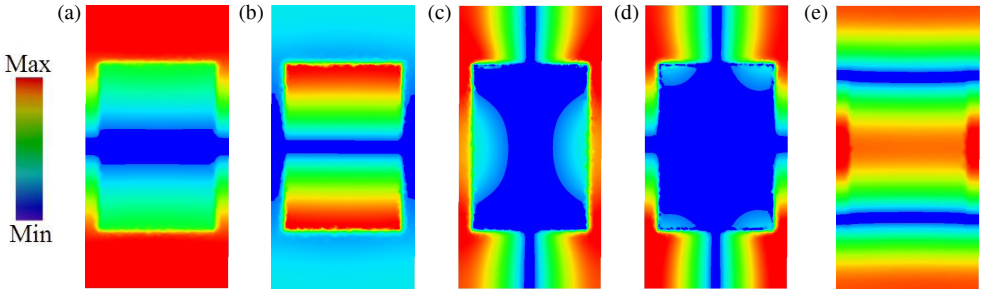

FIGURE 3. The electric field distribution of the first five modes in the CRPR. (a) Mode 1. (b) Mode 2. (c) Mode 3. (d) Mode 4. (e) Mode 5.

Here, m and n represent the mode indices along the x- and y-axis directions, respectively, while c denotes the speed of light in free space. The length-to-width ratio of the patch or SIW can effectively regulate the variation of multiple modes within each cavity [5]. Based on this concept, after determining the initial length-to-width ratio of one rectangular resonant structure, the length-to-width ratio of the other rectangular structure can be adjusted to achieve the resonance of three modes of CRPR at nearby frequencies. For example, when the length and width of the patch structure are 35 mm and 17.5 mm, respectively, by adjusting the length (L_3) and width (W_3) of the RSIW, the resonance frequency of the first five modes in CRPR can be tuned, as shown in Fig. 2. This relative control also provides more degrees of freedom for mode regulation in CRPR.

When $L = 35\,\text{mm}$, $W = 17.5\,\text{mm}$, $L_3 = 20\,\text{mm}$, and $W_3 = 14\,\text{mm}$ in the CRPR, the resonant frequencies of modes 2, 3, and 4 become closely spaced, thereby achieving a single-cavity triple-mode resonator. At this point, the electric-field distribution of the first five modes of the CRPR are shown in Fig. 3, with the unloaded quality factors (Qu) of the three resonant modes ideally being 349, 392, and 403, respectively. The substrate used is Roger 5880. Its relative permittivity is 2.2.

3. ANALYSIS OF THE PROPOSED SINGLE-CAVITY TRIPLE-MODE BPF BASED ON CRPR

A single-cavity triple-mode BPF is proposed based on modes 2, 3, and 4 of the CRPR and its feeding structure. The layout of the proposed filter is shown in Fig. 4(a), where the feeding structure includes a stepped impedance microstrip feedline and a coplanar waveguide (CPW) structure. The distance between the center feedline and the CRPR center is defined as D. The other two feedlines are symmetrically placed on two sides of the CRPR center, with their distance from the center denoted as L_2. All feedlines have the same width, denoted as W_1. The gap between the feedline structure and CRPR is L_1, and the slot-line dimensions in the CPW structure are denoted as g_1 and g_2. The coupling topology of the proposed single-cavity triple-mode BPF can be regarded as a "box-like" coupling topology,

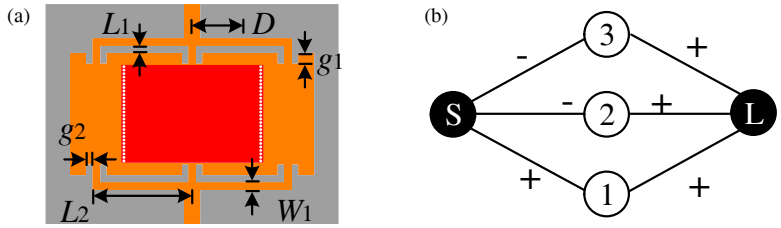

FIGURE 4. The proposed single-cavity triple-mode BPF based on CRPR. (a) Layout of the proposed filter (yellow or red: copper, white: metalized blind vias, gray: dielectric substrates) (b) "Box-like" coupling topology.

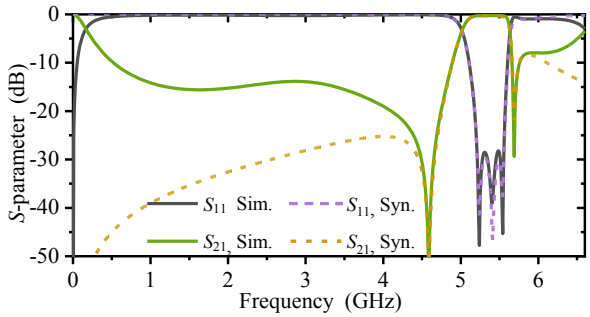

FIGURE 5. Simulation and synthesized S-parameters results of the proposed single-cavity triple-mode BPF based on CRPR.

as shown in Fig. 4(b), where S, L, 1, 2, and 3 represent the source, load, mode 2, mode 3, and mode 4, respectively.

To better demonstrate, a single-cavity triple-mode BPF with a f_0 of 5.35 GHz, a BW of 610 MH, and a return loss (RL) greater than 20 dB is designed. Using the High Frequency Structure Simulator (HFSS) full-wave electromagnetic simulation software, the simulated S-parameters of the BPF are shown in Fig. 5. The BPF has a fractional bandwidth (FBW) of 11.4 %, an insertion loss (IL) of 0.25 dB, and an RL of 28 dB. The frequency positions of the two FTZs are 4.58 GHz and 5.69 GHz, respectively. The main dimensions of the BPF that satisfy the engineering specifications are as follows: $W = 17.5$, $W_1 = 1.13$, $W_3 = 14$, $L = 35$, $L_1 = 1$, $L_2 = 14.3$, $L_3 = 20.01$, $g_1 = 1.5$, $g_2 = 0.9$, $d_1 = 0.4$, $d_2 = 0.1$, $D = 0$, $h_2 = 0.508$, $h_1 = 0.254$, all units: mm.

To further validate the effectiveness of the design method, the coupling matrix of the single-cavity triple-mode BPF based on CRPR is extracted. Based on this coupling matrix, the S-parameters are synthesized and compared with the simulation results. Fig. 5. shows the comparison between the synthesized and simulated results, indicating a high degree of consistency between them, thus further proving the accuracy of the design method. The extracted coupling matrix is as follows:

$$M=\begin{bmatrix} 0 & 0.7859 & -0.5282 & -0.2816 & 0 \\ 0.7859 & -0.5937 & 0 & 0 & 0.7859 \\ -0.5282 & 0 & 0.9499 & 0 & 0.5282 \\ -0.2816 & 0 & 0 & -1.0704 & 0.2816 \\ 0 & 0.7859 & 0.5282 & 0.2816 & 0 \end{bmatrix} \quad (3)$$

The proposed single-cavity triple-mode BPF features tunable FTZs and BW, providing high selectivity. As mentioned earlier, when the length-to-width ratio of the patch structure is fixed, adjusting the length and width of the RSIW can modify the resonant frequency of the specific mode of the CRPR. Therefore, as shown in Fig. 6(a), in the CRPR-based BPF, as the RSIW length (L_3) increases, the FTZs in the upper and lower stopbands shift to the left to varying degrees, and the BW decreases accordingly. As shown in Fig. 6(b), as the RSIW width (W_3) increases, the FTZs in the upper and lower stopbands shift to the right to varying degrees, and the BW decreases more significantly. Meanwhile, the rectangular factor of the BPF improves, and the suppression capability of the upper stopband is also enhanced. This is because increasing the RSIW width not only changes the resonant frequency of the specific mode but also effectively increases the excitation intensity of the feeding structure to mode 2, thereby altering the external quality factor (Qe). It is worth mentioning that the filtering characteristics can also be adjusted by fine-tuning the size parameters of the patch structure.

In addition, adjusting D and L_2 parameters in the filter can also achieve the fine-tuning of BPF S-parameters, as shown in Figs. 6(c) and (d). Essentially, this changes the Qe of each resonant mode, thereby affecting the matrix elements in the coupling matrix. Although the effect is relatively weak, it still serves as a supplementary method for tuning.

4. FABRICATION AND MEASUREMENT

To further validate the proposed design method for the single-cavity tri-mode filter, the filter is fabricated using printed circuit board (PCB) technology, and measurements are performed using a vector network analyzer (VNA). The physical prototype of the filter is shown in Fig. 7, and its measurement result is shown in Fig. 8. The f_0, IL, 3-dB BW, and RL of measured filter IV are 5.34 GHz, 1.86 dB (include the loss from the SubMiniature ver-

TABLE 1. Comparison with published bandpass filters.

Re	f_0 (GHz)	TP	IL (dB)	FTZ	FBW (%)	Size (λ g $\times$ λg)	T	Mode
[5]	5.78	4	1.45	2	3.5	0.45 × 0.82	Patch	HM
[8]	30	3	1.53	3	5.07	1.77 × 1.77	SIW	HM
[9]	4.4	3	1.44	0	25	0.65 × 0.65	Patch	FM
[10]	11.48	3	2.36	1	8.4	2.97 × 2.97	SIW	FM
[12]	5.52	3	1.67	1	22	1.01 × 1.01	QMSIW+Microstrip	FM
[13]	6.91	3	1.66	3	4.5	0.95 × 0.95	Hybrid cavity	HM
[14]	9.96	4	1.52	2	7.43	1.38 × 0.69	Hybrid cavity	FM
This work	5.34	3	1.98	2	11.61	0.49 × 0.95	hybrid cavity	HM

Re: References, TP: Transmission pole; T: Technique; FM: Fundamental mode; HM: Higher-order mode.

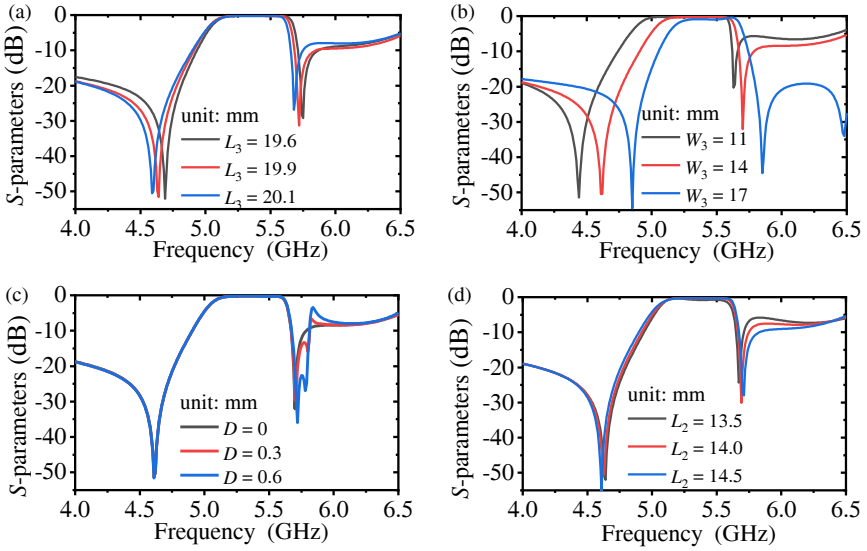

FIGURE 6. Controllable frequency locations of FTZs and BW by changing L_3 W_3, D and L_2, respectively. (a) L_3. (b) W_3 (c) D. (d) L_2.

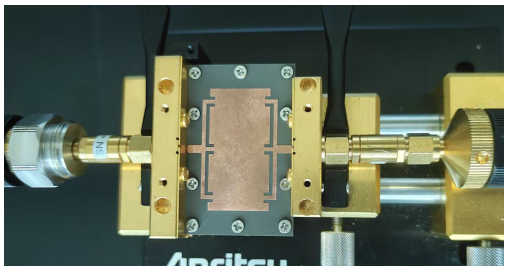

FIGURE 7. The prototype of the proposed single-cavity triple-mode BPF based on CRPR.

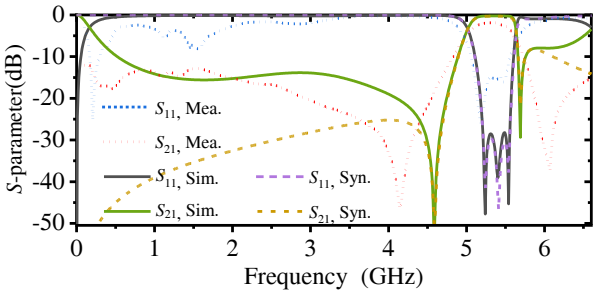

FIGURE 8. The measured S-parameters results of the proposed single-cavity triple-mode BPF based on CRPR.

sion A), 620 MH, and 14.7 dB, respectively. FTZs are located at 4.15 GHz and 6.07 GHz. As shown in Fig. 8, the simulation results, theoretical synthesized results, and actual measurement results are compared, and the three are consistent. The differences in the measurement results are mainly caused by the open radiation structure of the patch, processing tolerances, and measurement errors.

Table 1 compares the performance of the novel single-cavity triple-mode BPF based on the combined-type rectangular patch resonator with other planar cavity resonator filters from existing literature. Firstly, compared to [8, 10, 12–14], the proposed filter has a more compact size, and in contrast to [9, 10, 12], the proposed filter has more FTZs, demonstrating better selectivity. Moreover, the comparative experimental results strongly validate the superiority of the filter design scheme proposed in this paper, highlighting its broad application prospects in future research and providing a highly valuable solution for wireless communication systems.

5. CONCLUSION

In this paper, a single-cavity triple-mode BPF based on CRPR is proposed and studied. The BPF features tunable FTZs and BW, enabling high selectivity. By designing a specific example of a single-cavity triple-mode BPF, the consistency among theoretical analysis, simulation results, synthesis results, and measurement results demonstrates the effectiveness of this design method in achieving high selectivity, a relatively compact size, and easy integration of filters.

REFERENCES

[1] Zakharov, A. V. and S. M. Litvintsev, "Lumped-distributed resonators providing multiple transmission zeros in bandpass filters with simple and mixed couplings," *IEEE Transactions on Circuits and Systems I: Regular Papers*, Vol. 71, No. 8, 3502–3513, Aug. 2024.

[2] Sun, X., C. Rong, H. Gao, and M. Zhang, "A miniaturization dual-passband microwave filter based on load-coupled open stub lines," *Progress In Electromagnetics Research Letters*, Vol. 124, 17–21, 2025.

[3] Zhang, Z., G. Zhang, Z. Liu, W. Tang, and J. Yang, "Compact balanced bandpass filter based on equilateral triangular patch resonator," *IEEE Transactions on Circuits and Systems II: Express Briefs*, Vol. 69, No. 1, 90–93, Jan. 2022.

[4] Wang, X., N.-Y. Zhong, H. Li, J.-Y. Chu, H. Yang, X.-L. Yang, X.-W. Zhu, and W. Wu, "Miniaturized circular substrate integrated waveguide bandpass filter with flexible mixed coupling and wide stopband rejection," *IEEE Transactions on Circuits and Systems II: Express Briefs*, Vol. 71, No. 8, 3655–3659, Aug. 2024.

[5] Liu, Q., D. Zhou, X. Wang, M. Tang, D. Zhang, and Y. Zhang, "High-selective bandpass filters based on new dual-mode rectangular strip patch resonators," *IEEE Microwave and Wireless Components Letters*, Vol. 31, No. 10, 1123–1126, Oct. 2021.

[6] Yan, X. and W. Mu, "Square-coupled topological filter with an ideal rectangular coefficient facilitated by dual-cavity single-mode and single-cavity dual-mode SIW resonators," *Progress In Electromagnetics Research Letters*, Vol. 122, 1–7, 2024.

[7] Xu, Z., X. Sun, Y. Feng, Z. Wang, W. Zhong, and S. Fang, "Bandpass filters based on dual-mode slow wave substrate integrated waveguide cavities," *IEEE Microwave and Wireless Technology Letters*, Vol. 33, No. 8, 1131–1134, Aug. 2023.

[8] Liu, Q., D.-F. Zhou, K. Gong, J.-H. Wang, D.-W. Zhang, and B.-H. Ma, "Dual-and triple-mode single-layer substrate-integrated waveguide filters based on higher-order modes for millimeter-wave applications," *IEEE Transactions on Circuits and Systems II: Express Briefs*, Vol. 71, No. 4, 1994–1998, Apr. 2024.

[9] Gong, K., S. Ma, C. Fan, J. Sun, J. Han, Y. Liu, and Q. Liu, "Miniaturised single-layer bandpass filters using triple and quad-mode patch resonators," *IET Microwaves, Antennas & Propagation*, Vol. 17, No. 13, 1015–1022, Oct. 2023.

[10] Chen, C. and Q. Ji, "Triple-mode dual-band bandpass filter based on cross-shaped substrate integrated waveguide," *Electronics Letters*, Vol. 55, No. 3, 138–140, Feb. 2019.

[11] Liu, B.-G. and C. Cheng, "Compact wide-stopband bandpass filter using fsiw-patch triple-mode resonator," *Microwave and Optical Technology Letters*, Vol. 66, No. 1, e33929, Jan. 2024.

[12] Li, M., Q. Ji, C. Chen, W. Chen, and H. Zhang, "A triple-mode bandpass filter with controllable bandwidth using QMSIW cavity," *IEEE Microwave and Wireless Components Letters*, Vol. 28, No. 8, 654–656, Aug. 2018.

[13] Qian, H., D.-W. Zhang, Q. Liu, X. Wang, H.-L. Deng, H.-H. Xu, L.-C. Yang, and D.-F. Zhou, "Highly-selective bandpass filter with enhanced stopband performance based on higher-order triple-mode folded-embedded single-cavity," *Microelectronics Journal*, Vol. 156, 106568, Feb. 2025.

[14] Jiao, M. R., F. Zhu, P. Chu, W. Yu, and G. Q. Luo, "Compact hybrid bandpass filters using substrate-integrated waveguide and stripline resonators," *IEEE Transactions on Microwave Theory and Techniques*, Vol. 72, No. 1, 391–400, Jan. 2024.